Electrocatalysis in Nucleic Acid Molten Salts†

Anthony M. Leone,‡ Dominic O. Hull, Wei Wang, H. Holden Thorp,* and Royce W. Murray*

Kenan Laboratories of Chemistry, University of North Carolina, Chapel Hill, North Carolina 27599-3290

Received: March 5, 2004; In Final Form: April 16, 2004

This paper describes redox chemistry in semisolid molten salts ionic liquids of DNA in which the counterions of the phosphates are redox-active metal complexes with bipyridine ligands labeled with MW 350 poly(ethylene glycol) (PEG) "tails", e.g., $M(bpy_{350})_3DNA$ (where M = Co, Ni, and bpy_{350} = 4,4′-$(CH_3(OCH_2CH_2)_7OCO)_2$-2,2′-bipyridine). Other redox-active metal complexes are added to the $M(bpy_{350})_3DNA$ melt: (a) the PEG-tailed metal bipyridine complexes $Fe(bpy_{350})_3(ClO_4)_2$ and $Ru(bpy_{350})_3(ClO_4)_2$ and (b) the nontailed complexes $Os(bpy)_3Cl_2$ (bpy = 2,2′-bipyridine) and $Os(bpy)_2dppzCl_2$ (dppz = dipyridophenazine). In example a, electrogeneration of the powerful oxidizers $[Fe(bpy_{350})_3]^{3+}$ and $[Ru(bpy_{350})_3]^{3+}$ gives microelectrode voltammetry indicative of electrocatalytic oxidation of DNA base sites. Since physical diffusion of the metal complexes is slow in the viscous semisolids (and that of DNA is nil), the rate of electron hopping between the base sites of the DNA becomes a significant contributor to the overall charge transport rate, as deduced from analysis of the voltammetry. DNA base site self-exchange rate constants of 1.1×10^6 and 1.8×10^6 s^{-1} are estimated from measurements using $Fe(bpy_{350})_3^{3+}$ and $Ru(bpy_{350})_3^{3+}$ oxidants, respectively. In example b, a complex known to be a DNA intercalator in aqueous solutions is found to not be an intercalator in the DNA molten salt environment, as deduced from measurements showing the physical diffusion coefficients of aqueous nonintercalator $Os(bpy)_3Cl_2$ and aqueous intercalator $Os(bpy)_2dppzCl_2$ to be indistinguishable in the $M(bpy_{350})_3DNA$ melt.

Introduction

Our laboratory has extensively investigated semisolid ionic liquids (e.g., room-temperature molten salts, in classical, conventional nomenclature) in which one ion partner of the melt is redox-active and one partner is attached to one or more low molecular weight, methoxy-terminated, poly(ethylene oxide) chains, i.e., the ion has "PEG tails".[1−4] Such PEG labeling has been effective in forming ionic liquids from substances as chemically diverse as ferrocyanide[5] and DNA.[6,7] Because physical diffusion in these viscous materials is very slow, voltammetrically initiated charge transport tends to be dominated by electron hopping in the mixed-valent phase generated around the working electrode. This property makes these novel phases attractive media in which to study the fundamentals of bimolecular self-exchange electron transfers in semisolid molecular environments and is used in the present study to estimate base−base electron-transfer rates along DNA chains.

We recently described[6] molten salts of DNA in which the DNA polyanion had metal complex counterions bearing bipyridine ligands labeled (Figure 1) with MW 350 poly(ethylene glycol) (PEG) tails, e.g., $Co(bpy_{350})_3DNA$ (where bpy_{350} = 4,4′-$(CH_3(OCH_2CH_2)_7OCO)_2$-2,2′-bipyridine). Numerous electron-transfer schemes have been suggested for using DNA base pairs as templates for self-assembly,[8,9] computing,[10] wiring,[11] and analytical measurements[9,12−15] and deploying such guided functions within an ionically and electronically conductive medium containing DNA is an intriguing goal. However, central to such ideas is an understanding of how fast, mechanistically and dynamically, electrons can flow in an assembly based on DNA as a structural element.[16,17,18] For electron transport within a DNA duplex to be apparent, the other alternative modes of electron transport (i.e., by physical diffusion) must be slowed,[1−4]

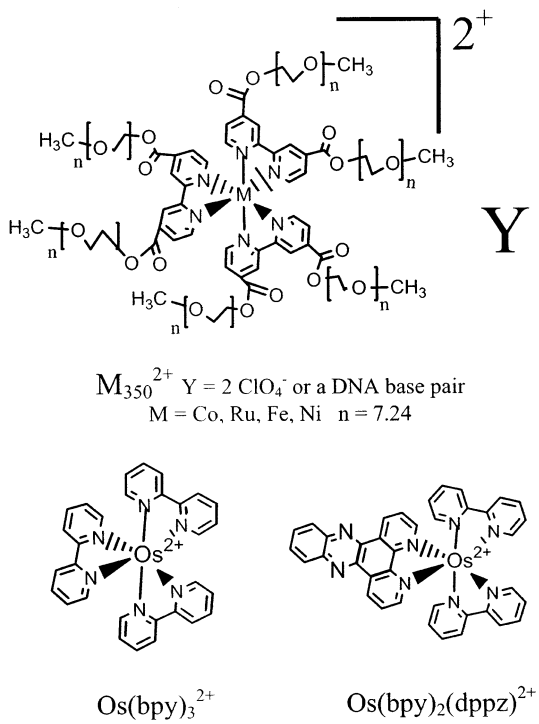

Figure 1. Structures of M_{350}^{2+} (M = Co, Fe, Ni, or Ru) molten salts where the counterion, Y, can be two ClO_4^- or two nucleotide phosphates of a DNA molecule. All DNA molten salts discussed here contain defined added equivalents of $M_{350}(ClO_4)_2$ (M = Co, Fe, or Ru). Structures of $Os(bpy)_3^{2+}$ and $Os(bpy)_2dppz^{2+}$ where Cl^- is the counterion.

† Part of the special issue "Tomas Baer Festschrift".

‡ Present address: Merck Research Laboratories, West Point, PA 19486.

10.1021/jp048995l CCC: $27.50
Published on Web 06/04/2004

SCHEME 1: Electrocatalysis in DNA Molten Salts[a]

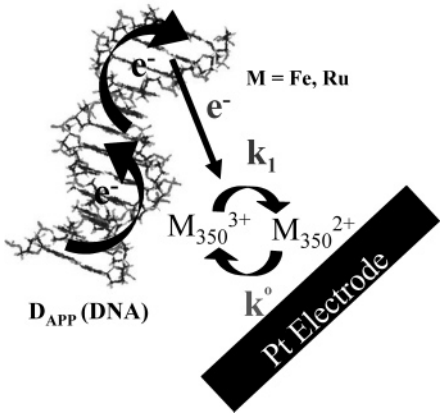

[a] The electrocatalytic cycle is initiated with oxidation of the M_{350}^{2+} mediator at the electrode surface having a rate constant of $k°$. The M_{350}^{3+} subsequently oxidizes a guanine or adenine base in DNA with rate constant k_1. The electron hopping among the DNA bases replenishes the oxidized base site, giving a D_{APP} for DNA and associated rate constant for electron hops of k_{EX}.

suggesting that semisolid media containing DNA would allow evaluation of the base−base electron transport.

In this paper, electron-transfer reactions of DNA are observed in an electrocatalytic scheme where PEG-tailed metal bipyridine complexes $Fe(bpy_{350})_3(ClO_4)_2$ and $Ru(bpy_{350})_3(ClO_4)_2$ (M_{350}) are added to $Co(bpy_{350})_3$DNA melts. The strongly oxidizing M^{3+} states of the Fe and Ru complexes are electrochemically generated (with heterogeneous electron-transfer rate constants $k°$, eq 1) and react with DNA base sites (Scheme 1, guanine and adenine, with rate constants k_1, eq 2) according to the electrocatalytic scheme

$$M_{350}^{2+} \rightarrow M_{350}^{3+} + e^- \quad (1)$$

$$M_{350}^{3+} + DNA \rightarrow M_{350}^{2+} + DNA^+ \quad (2)$$

In such a scheme, the electrochemical currents for waves described by eq 1 become enhanced by the recycling of M_{350}^{2+} produced in eq 2, and the electrochemically detected supply of M_{350}^{3+} is accordingly diminished according to well-established principles.[19] In conventional electrocatalysis, the electron donor (DNA in this case) continues to diffuse toward the electrode, replenishing its oxidizable components. However, in the present case, the physical diffusion coefficient of DNA ($D_{PHYS,DNA}$) is nil, so any experimental indication that DNA "diffuses" must be interpreted as an ability of the DNA to transport charge within itself, namely by site−site electron self-exchange between mixed-valent base pair sites.[16−18] Evidence for this process is furnished by an analysis of the electrocatalytic currents.

A second purpose of the present investigation was to ask whether metal complexes that are aqueous DNA intercalators (such as $Os(bpy)_2(dppz)Cl_2$, Figure 1) could be so in the semisolid $Co(bpy_{350})_3$DNA environment. Intercalated metal complexes have been useful in studying electron transfers along the DNA helix.[17] We therefore introduced the non-PEG-tailed complexes $Os(bpy)_3Cl_2$ (a nonintercalator) and $Os(bpy)_2(dppz)Cl_2$ into the $Co(bpy_{350})_3$DNA melt. Voltammetry of these complexes, which are soluble in the melts up to about 5%, demonstrates their diffusive mobility, which in turn estimates whether they are complexed with the immobile DNA chains.[20] The two complexes give equivalent diffusivities, indicating that intercalation is weak or absent in the semisolid melts.

Experimental Section

Synthetic reagents (Sigma Aldrich) were purified before use. Millipore ultrapure water was used in all experiments. Herring testes DNA (Sigma) was used unless otherwise noted. Elemental analysis was performed by EAI Co. Aqueous molar concentrations were calculated from optical absorbances on the basis of the following molar absorbances: $\epsilon_{306} = 31\,700\ M^{-1}\ cm^{-1}$ for $Co_{350}(ClO_4)_2$, $\epsilon_{548} = 16\,200\ M^{-1}\ cm^{-1}$ for $Fe_{350}(ClO_4)_2$, $\epsilon_{327} = 27\,800\ M^{-1}\ cm^{-1}$ for $Ni_{350}(ClO_4)_2$, $\epsilon_{468} = 25\,800\ M^{-1}\ cm^{-1}$ for $Ru_{350}(ClO_4)_2$, $\epsilon_{490} = 12\,900\ M^{-1}\ cm^{-1}$ $Os(bpy)_3Cl_2$, $\epsilon_{476} = 16\,900\ M^{-1}\ cm^{-1}$ for $Os(bpy)_2(dppz)_3Cl_2$, and $\epsilon_{260} = 6600\ M^{-1}\ cm^{-1}$ for herring testes DNA, where the concentration of nucleic acids is expressed in nucleotide phosphates. $Os(bpy)_3Cl_2$ and $Os(bpy)_2(dppz)_3Cl_2$ were prepared according to published procedures.[20,21] Co_{350}DNA was prepared as described previously;[7] Ni_{350}DNA was prepared by an analogous procedure.

The bpy-tailed complexes $Co_{350}(ClO_4)_2$, $Fe_{350}(ClO_4)_2$, and $Ni_{350}(ClO_4)_2$ (Figure 1) were prepared as previously described.[4] $Ru_{350}(ClO_4)_2$ was prepared with a slight modification to the previous procedure,[3] as follows: 1 equiv of $RuCl_3$ was added to 3.5 equiv of the tailed bpy-ligand in a minimal amount of ethylene glycol. Then 3.1 equiv of $AgClO_4$ was added to the mixture along with 1 equiv of benzoquinone, and the mixture was refluxed under Ar for 1.5 h, forming a dark red solution that was filtered through Celite to remove AgCl and then dialyzed for 48 h in a 1000 MW (cutoff) membrane to remove ethylene glycol and other small-molecule impurities. Repeated extraction with diethyl ether removed excess tailed ligand from this product; another brown-colored impurity was removed using a 13 in. Brockman I basic alumina column, eluting with acetonitrile.

Molecular melts containing mixtures of M_{350}DNA (M = Co, Ni) and $M_{350}(ClO_4)_2$ (M = Co, Ni, Fe, Ru) were prepared by mixing aqueous solutions of the indicated components, determining their actual concentrations by absorption spectrophotometry. After thorough mixing, water was removed under vacuum. Electrocatalysis experiments were conducted on Co_{350}DNA melts containing equimolar quantities (in metal ion) of $Co_{350}(ClO_4)_2$ and either $Fe_{350}(ClO_4)_2$ or $Ru_{350}(ClO_4)_2$ (i.e., the ratio Co_{350}DNA to $Co_{350}(ClO_4)_2$ to $M_{350}(ClO_4)_2$ (M = Fe, Ru) was always 1:1:1). Pycnometry gave a density of 1.25 g/mL for this melt, which corresponds to a total metal complex concentration $[M_{350}^{2+}]_{Total} = 0.40$ M. $Ni_{350}(ClO_4)_2$ was added to Ni_{350}DNA melts in a 3:1 mole ratio.

DNA molten salts containing $Os(bpy)_3Cl_2$ and $Os(bpy)_2(dppz)_3Cl_2$ were also prepared by mixing aqueous solutions and drying. To prepare, for example, 3 mM $Os(bpy)_3Cl_2$ in the melt Ni_{350}DNA + $3Ni_{350}(ClO_4)_2$, 209 μL of 3.83 mM Ni_{350}DNA (0.8 μmol), 198 μL of 12.1 mM $Ni_{350}(ClO_4)_2$ (2.4 μmol), and 292 μL of 0.082 mM $Os(bpy)_3Cl_2$ (24 nmol) were mixed, and the water was removed under vacuum.

Electrochemical Experiments. The melts were studied as films that had been cast onto a three-electrode (wire tips) platform as previously described.[1−4] The films were predried under vacuum at 70 °C for at least 12 h and were maintained at 67 °C and 10^{-3} Torr vacuum during voltammetry, which was performed with an in-house-built low current potentiostat and software. The working microelectrode was a 5.3 μm radius Pt disk. The reference electrode was a quasireference silver wire tip unless otherwise noted. Diffusion coefficients for $Os(bpy)_3Cl_2$ and $Os(bpy)_2(dppz)_3Cl_2$ in the melts were determined by chronoamperometry, using potential steps from the foot to the plateaus of the $Os^{3+/2+}$ oxidation waves and plotting current−

time data according to the Cottrell equation.[19,22] All results are averages of at least three measurements on independent films.

Digital Simulations. Simulations of voltammetric responses were carried out using the DigiSim software package (BAS).[23] Microelectrode areas were determined from steady-state currents for ferrocene oxidation in an acetonitrile/Bu_4NClO_4 solution. The DNA employed (herring testes) contained equal populations of the four nucleotide bases, but only guanine and adenine were oxidizable by Fe_{350}^{3+}, as determined separately by stopped-flow absorption spectrophotometry as described below. Simulations therefore used one-half of the actual DNA concentration in the melt to reflect the concentration of redox-active bases (guanine and adenine). The concentration of the electrocatalytic oxidants [$Fe_{350}(ClO_4)_2$ and $Ru_{350}(ClO_4)_2$] was lower than the percolation threshold for $M^{3+/2+}$ hopping, so these species transported charge solely by physical diffusion. The physical diffusion coefficient of PEG-tailed metal complexes used in all simulations was measured from the $Co_{350}^{3+/2+}$ wave; the result, 1.7×10^{-10} cm^2/s, agreed with a previous measurement in Co_{350}DNA + $2Co_{350}(ClO_4)_2$ (1.7×10^{-10} cm^2/s).[7] Melt ionic conductivity, ρ^{-1}, was measured with ac impedance, and melt uncompensated resistance (R_{UNC}) was calculated[24] from the microdisk equation $R_{UNC} = \rho/4\pi r$, where ρ^{-1} was 5.54×10^{-6} and 1.21×10^{-5} S/cm and R_{UNC} = 27.1 and 12.4 MΩ for the Co_{350}DNA + $2M_{350}(ClO_4)_2$ melt and the undiluted $M_{350}(ClO_4)_2$ melt, respectively. Apparent heterogeneous electron-transfer rate constants for the $Fe_{350}^{3+/2+}$ and $Ru_{350}^{3+/2+}$ complexes were determined by fitting cyclic voltammograms in pure $Fe_{350}(ClO_4)_2$ and $Ru_{350}(ClO_4)_2$ melts, giving $k° = 3.3 \times 10^{-4}$ and 2.1×10^{-4} cm/s, respectively. These fits also took account of a parasitic reaction in the melts that reconverts M^{3+} to M^{2+} (known to also occur in solution):[13]

$$M_{350}^{2+} \rightarrow M_{350}^{3+} + e^- \qquad (3)$$

with a rate constant k_f ranging from 0.08 to 0.3 s^{-1}. These values for $k°$ and k_f were assumed to be the same in melts containing DNA. The rate constant for DNA oxidation (eq 2, k_1) and the apparent DNA diffusion coefficient were the only adjustable variables in the simulations shown in the figures.

Stopped-Flow Spectrophotometry. The rates of oxidation of the individual nucleotides in acetonitrile solutions were determined for comparison to the melt results. The free acid mononucleotides of dGMP, dAMP, or TMP were neutralized with 2 equiv of $Bu_4N^+OH^-$ to solubilize them in acetonitrile, as previously described.[25]

Stopped-flow experiments were carried out at 25 ± 1 °C out using an On Line Instrument Systems OLIS RSM-1000 according to the methods of Weatherly et al.,[25] where the reaction was monitored at λ_{max} = 540 nm of the Fe_{350}^{2+} form of the metal complex. The oxidized complex, Fe_{350}^{3+}, was freshly prepared for each experiment by bulk electrolysis in a 0.05 M $LiClO_4/CH_3CN$ solution. The $(Bu_4N^+)_2$dGMP solution was 1 mM in 0.05 M $LiClO_4/CH_3CN$. Ru_{350}^{3+} was too unstable for these measurements. The second-order reaction rate constants for

$$Fe^{3+} + DNA \rightarrow Fe^{2+} + DNA_{ox} \qquad (4)$$

were determined by global analysis.[26]

Results and Discussion

Molten salts of Co_{350}DNA in which the populations of DNA base pairs and Co complex are stoichiometrically equal (and no other mobile ions are present) exhibit extremely low ionic conductivity and no useful voltammetric responses.[7] This situation exists because the physical diffusivity of the DNA (average molecular mass 70 kDa) is nil, which imposes an electroneutrality constraint on electrochemical reactions. Therefore, the M_{350}DNA (M = Co, Ni) melts discussed here always contain some added quantity of the ClO_4^- salt of one or more PEG-tailed metal complexes, $M_{350}(ClO_4)_2$ (M = Co, Ni, Fe, Ru, Figure 1).

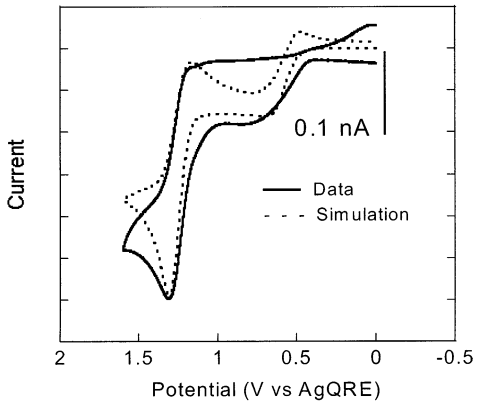

Figure 2. Cyclic voltammetry (solid) and digital simulations (dashed) of Co_{350}DNA + 1 equiv each of $Co_{350}(ClO_4)_2$ and $Fe_{350}(ClO_4)_2$. [Co_{350}^{2+}] = 0.27 M, [Fe_{350}^{2+}] = 0.13 M, and [DNA] = 0.26 M. Voltammetry measured at 67 °C on 5.1 μm radius Pt microelectrode at scan rate = 10 mV/s. Digital simulation parameters were R_{UNC} = 27 MΩ, C_{DL} = 30 pF, α = 0.5, $k° = 3.3 \times 10^{-4}$ cm/s, $k_f = 0.1$ s^{-1}, $k_1 = 500$ M^{-1} s^{-1}, $D_{PHYS} = 1.1 \times 10^{-10}$ cm^2/s, DNA $D_{APP} = 5.3 \times 10^{-9}$ cm^2/s.

Electrocatalytic Oxidation of DNA in PEG-Based Molten Salts. The formal potentials of the $Fe_{350}^{3+/2+}$ and $Ru_{350}^{3+/2+}$ couples in acetonitrile, 1.1 and 1.5 V vs Ag/AgCl, respectively, are sufficiently positive that these M_{350}^{3+} complexes oxidize guanine and (more slowly) adenine sites in DNA. Electrocatalytic waves have been observed in both melt[6] and dilute aqueous solution[12,27] mixtures of such metal complexes with DNA. Figure 2 shows voltammetry of the 1:1:1 (mole ratio) melt Co_{350}DNA + $Co_{350}(ClO_4)_2$ + $Fe_{350}(ClO_4)_2$. The first oxidation step is for the $Co_{350}^{3+/2+}$ oxidation; note that the $Fe_{350}^{3+/2+}$ currents for the second wave at 1.3 V are 3-fold larger, even though this complex is at one-half the concentration of the Co complex. In contrast to our earlier experiment,[5] the $Fe_{350}(ClO_4)_2$ complex was employed at a concentration much lower than the percolation threshold for significant charge transport by electron hopping between Fe_{350}^{3+} and Fe_{350}^{2+}. The percolation threshold was established as ca. 0.4 mole fraction of the $Fe_{350}(ClO_4)_2$ complex [in $Co_{350}(ClO_4)_2$ or $Ni_{350}(ClO_4)_2$] in previous[2] work. To emphasize this point, Figure 3 shows voltammetry of a 2.4:1 (mole ratio) melt mixture of $Co_{350}(ClO_4)_2$ + $Fe_{350}(ClO_4)_2$ that contains no DNA. The $Fe_{350}^{3+/2+}$ wave in this mixture is smaller than the $Co_{350}^{3+/2+}$ wave by roughly a factor of 2, as expected for purely physical diffusion transport of the former.

The 6-fold enhanced current (relative to Co) at +1.3 V in Figure 2 is therefore attributed to electrocatalytic recycling of Fe_{350}^{2+} due to the oxidation of DNA (eq 2). Consistent with this interpretation, the reverse wave for reduction of Fe_{350}^{3+} is less than one-half as large as the oxidation current. Figure 4 shows an analogous experiment at a 1:1:1 (mole ratio) melt Co_{350}DNA + $Co_{350}(ClO_4)_2$ + $Ru_{350}(ClO_4)_2$, using now the more oxidatively potent[12,27,28] Ru_{350}(III/II) couple. The enhancement of Ru_{350}^{2+} oxidation current at +1.4 V is now 10-fold (relative to Co), and the reverse Ru_{350}^{3+} reduction wave is almost absent.

The electrocatalytic currents of Figures 2 and 4 diminish upon repeated scans over the same potential intervals, although they

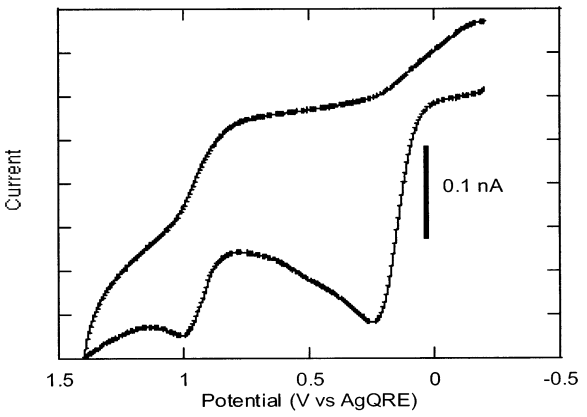

Figure 3. Cyclic voltammetry of a $Co_{350}(ClO_4)_2$ and $Fe_{350}(ClO_4)_2$ mixture. $[Co_{350}^{2+}] = 0.31$ M, $[Fe_{350}^{2+}] = 0.13$ M. Voltammetry measured at 67 °C on 5.1 μm radius Pt microelectrode at scan rate = 10 mV/s.

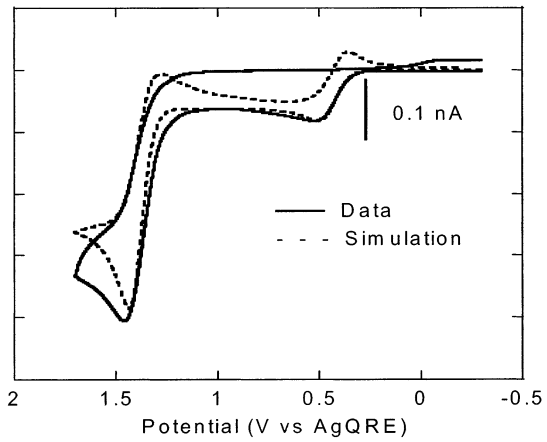

Figure 4. Cyclic voltammetry (solid) and digital simulations (dashed) of Co_{350}DNA + 1 equiv each of $Co_{350}(ClO_4)_2$ and $Ru_{350}(ClO_4)_2$. $[Co_{350}^{2+}] = 0.27$ M, $[Ru_{350}^{2+}] = 0.13$ M, and [DNA] = 0.26 M. Voltammetry measured at 67 °C on 5.3 μm radius Pt microelectrode at scan rate = 10 mV/s. Digital simulation parameters were R_{UNC} = 27 MΩ, C_{DL} = 30 pF, $\alpha = 0.5$, $k° = 2.0 \times 10^{-4}$ cm/s, $k_f = 0.1$ s^{-1}, $k_1 = 700$ M^{-1} s^{-1}, $D_{PHYS} = 1.1 \times 10^{-10}$ cm^2/s, DNA $D_{APP} = 9.0 \times 10^{-9}$ cm^2/s.

remain larger than the original $Co_{350}^{3+/2+}$ currents (Figure S-1). The drop in the electrocatalytic currents is expected given the insignificant DNA physical diffusion rate and that fact that the oxidation of its nucleotide sites is ultimately an irreversible process. The observation that the electrocatalysis is somewhat persistent over multiple scans indicates that in some manner the DNA base sites are becoming replenished. The $Co_{350}^{3+/2+}$ wave is suppressed upon continued potential scanning, which suggests that some reaction products foul the Pt electrode surface. Because of these effects, analyzing the voltammetry at a wide variety of potential scan rates was not feasible,[29] and we relied instead on simulations of the electrocatalytic voltammetry and comparative stopped-flow spectrophotometry to evaluate the electrocatalytic processes.

A stopped flow spectrophotometric evaluation of Fe_{350}^{3+} oxidation of Bu_4N^+ salts of dilute solutions of the deoxyribose nucleotide monophosphates in acetonitrile is shown in Figure 5. In this case, the absorbance band for Fe_{350}^{2+} at 544 nm increases as Fe_{350}^{3+} oxidizes $(Bu_4N^+)_2$dAMP. Fitting of the kinetic trace produces electron-transfer rate constants for one-electron oxidation[25] of guanine and adenine of $(1.7 \pm 0.3) \times 10^4$ and $(1.0 \pm 0.2) \times 10^3$ M^{-1} s^{-1}, respectively. Similar experiments with Fe_{350}^{3+} and the pyrimidine bases $(Bu_4N^+)_2$-

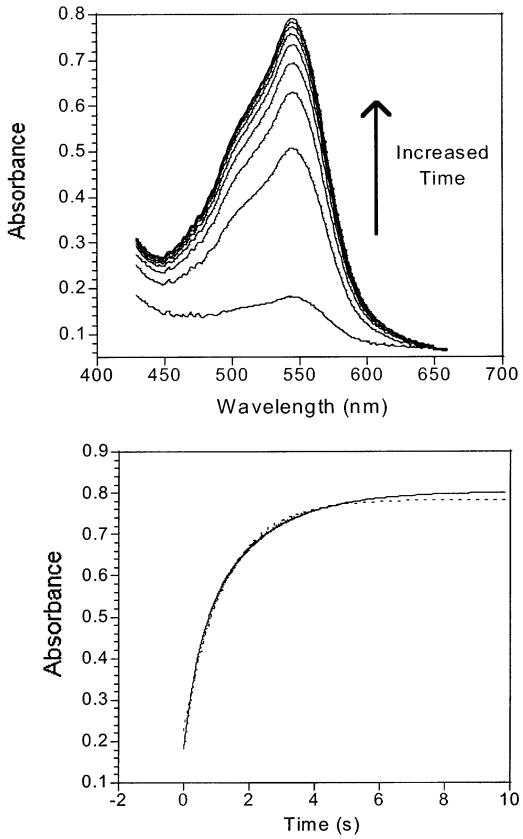

Figure 5. (A) Results of stopped-flow spectrophotometry for the reaction of 500 μM $(Bu_4N^+)_2$dAMP with 20 μM Fe_{350}^{3+} in 50 mM $LiClO_4$ acetonitrile solution. (B) Fe_{350}^{2+} absorbance at 544 nm vs time data (solid curve) from part A and fit (dashed curve). Data fits provided average rate constants of $1.0 \pm 0.2 \times 10^3$ M^{-1} s^{-1} and $1.7 \pm 0.3 \times 10^4$ M^{-1} s^{-1} for one-electron oxidation of dAMP and dGMP (not shown), respectively.

dCMP and $(Bu_4N^+)_2$TMP showed no appreciable reduction of the Fe_{350}^{3+} on a time scale comparable to the $(Bu_4N^+)_2$dGMP and $(Bu_4N^+)_2$dAMP experiments. Guanine and adenine can therefore be regarded as the reactive species. Since the DNA employed in the molten salt experiments contained equimolar quantities of the four native nucleotides, the concentration of reactive DNA sites was taken as one-half the actual concentration of DNA nucleotides for the purpose of the voltammetric simulations.

Electron-transfer rates in molten salts are intimately connected with rates of physical diffusive transport and have been hypothesized to be limited by the rate of ionic atmosphere relaxation.[7,30] It would not be surprising then to find that the M_{350}^{3+} + DNA electron-transfer rate in the molten salt (eq 2) is slower than the rate in fluid solution determined by stopped-flow, since D_{PHYS} is approximately 5 orders of magnitudes smaller in the melt. The stopped flow data can therefore be regarded as the upper limit of the rate constant of eq 2 in the melt.

The voltammetric simulations employed independent initial estimates of all of the parameters that should influence the electrocatalysis. These include the electrode area, the M_{350}^{2+} and DNA concentrations, the metal complex physical diffusion coefficients (M_{350}^{2+} $D_{PHYS} = 1.1 \times 10^{-10}$ cm^2/s),[7] the heterogeneous electron-transfer rate constants ($k°$) for the one-electron oxidations of the Fe_{350}^{2+} (3.3×10^{-4} cm/s) and Ru_{350}^{2+} (2.1×10^{-4} cm/s) complexes, the rate constant of the parasitic reaction (k_f) that consumes some of the electrogenerated M_{350}^{3+} (0.085 and 0.34 s^{-1}, respectively, for Fe and Ru), and k_1 for eq 2

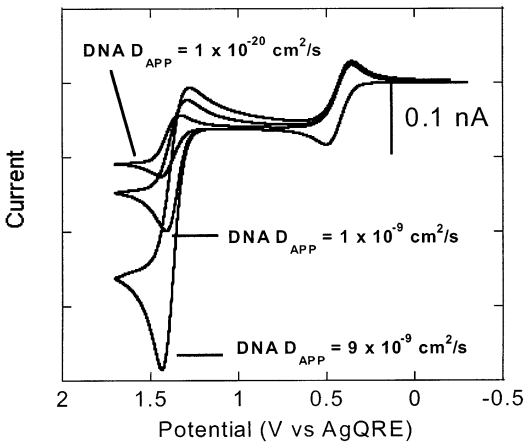

Figure 6. Digital simulations illustrating the influence of DNA D_{APP} on $Ru^{3+/2+}$ voltammetric response. All simulation parameters were, for consistency, the same as in Figure 4m except for the DNA $D_{APP,DNA}$, which was varied from 1.0×10^{-20} cm^2/s to 9.0×10^{-9} cm^2/s. Digital simulation parameters were $R_{UNC} = 27$ MΩ, $C_{DL} = 30$ pF, $\alpha = 0.5$, $k^\circ = 2.0 \times 10^{-4}$ cm/s, $k_f = 0.1$ s^{-1}, $k_1 = 700$ M^{-1} s^{-1}, $D_{PHYS} = 1.1 \times 10^{-10}$ cm^2/s.

estimated by stopped-flow measurements. The values of k° and k_f were obtained by fitting cyclic voltammograms of the pure $M_{350}(ClO_4)_2$ molten salts. In these initial simulations, the diffusivity of the DNA was the only parameter not measured independently, and from previous voltammetry[14] it was expected to be very small.

Figure 6 shows a voltammogram calculated using the above parameters and assuming that the physical diffusion rate of the DNA was extremely slow ($D_{PHYS,DNA} = 1 \times 10^{-20}$ cm^2/s). The value used for k_1 was varied from 10 to 10^4 M^{-1} s^{-1} with little effect on the simulation. The simulation at $D_{PHYS,DNA} = 1 \times 10^{-20}$ cm^2/s did not produce significant electrocatalytic current enhancement;[31] the calculated Fe_{350}^{2+} oxidation current is even smaller than that for the Co_{350}^{2+} oxidation and lacks the irreversible features characteristic of an electrocatalytic process. The absence of significant electrocatalysis in this simulation is due to depletion of reactive base sites in DNA lying within the Fe_{350}^{3+} diffusion layer; the specification of $D_{PHYS,DNA} = 1 \times 10^{-20}$ cm^2/s prevents the diffusive replenishment of unoxidized bases and hence an increased oxidative current.

The absence of electrocatalytic current suggested a nonzero flux of unoxidized DNA base sites toward the electrode surface. Figure 6 shows that assuming much higher *apparent* diffusivities for DNA, up to $D_{APP,DNA} = 9 \times 10^{-9}$ cm^2/s, does in fact produce electrocatalytic currents that are multiples of the Co_{350}^{2+} oxidation currents, resembling the voltammetry of Figures 2 and 4. The dashed, simulated voltammograms in Figures 2 and 4 were obtained by varying the apparent DNA diffusion coefficient $D_{APP,DNA}$ and the rate constant for the M_{350}^{3+} + DNA reaction (eq 2). The former has the predominant effect on the electrocatalytic oxidation current, as in Figure 6. The results obtained for the combined best fit to the electrocatalytic oxidation current and the reverse reduction wave were, for the Fe_{350}^{3+} reaction (Figure 2), $D_{APP,DNA} = 5.3 \times 10^{-9}$ cm^2 s^{-1} and $k_1 = 500$ M^{-1} s^{-1}, and for the Ru_{350}^{3+} reaction (Figure 4), $D_{APP,DNA} = 9 \times 10^{-9}$ cm^2 s^{-1} and $k_1 = 700$ M^{-1} s^{-1}.

The major result of Figures 2 and 4 is that one must assume that DNA is capable of transporting charge at a much faster pace than it can physically diffuse. This process can occur by electron self-exchange reactions between adenine or guanine radical cations along the DNA duplex. Apparent diffusion coefficients on the order of 10^{-9} cm^2/s are typical in the PEG-based molten salts, where contributions to charge transport from electron hopping are common.[1−4] It is therefore possible to make a crude estimate of the DNA electron hopping rate constant k_{EX} (s^{-1}) from the $D_{APP,DNA}$ results, using the relation for diffusion in one dimension,[32]

$$D_{APP,DNA} = k_{EX}\delta^2 \quad (5)$$

where δ is the average hop length. If one assumes that G's and A's can exchange electrons only between themselves and each other, then statistically two of the four sites in a two base pair sequence are reactive. Assuming that the hop can be along a chain or diagonally across the helix,[33] we choose an average hop distance of $\delta = 7$ Å based on 3.4 Å base separation and 20 Å helical diameter. This produced estimates (at 67 °C) of $k_{EX} = 1 \times 10^6$ s^{-1} and 2×10^6 s^{-1} from the Fe and Ru data in Figures 2 and 4, respectively. These estimates of the rate constants for electron hopping along the interior of the DNA stack are several orders of magnitude larger than the value of k_1, which is the reason for the large effect of $D_{APP,DNA}$ on the voltammetric simulations, relative to that of k_1.

Substantial variation[16,17] exists among the literature rate data on DNA base−base electron transfers, ranging from 10^6 to 10^{11} s^{-1}. Molecular dynamics,[18] DNA base sequences, and structure fluctuations[34] are widely accepted to impact the rate. The DNA used here, while known to retain double helical structure,[6] is comprised of large heterogeneous sequences and is otherwise ill-characterized. It is additionally possible that ionic atmosphere relaxation[35] phenomena influence the DNA electron hopping rate. We have shown that ionic atmosphere relaxation can dominate electron-transfer rates in semisolid media;[7,30,36] such control in the present case would mean that the k_{EX} results above are lower limits of the intrinsic electron-transfer rate. Measurements given below show, however, that the physical diffusion of dilute, nontailed metal complexes in a 1:3 (mole ratio) Ni_{350}-DNA + $Ni_{350}(ClO_4)_2$ melt at 67 °C is about 10^{-8} cm^2/s. This result is probably a lower limit for the value of the ClO_4^- counterion diffusion coefficient in the Co_{350}DNA + $Co_{350}(ClO_4)_2$ + $Fe_{350}(ClO_4)_2$ melts, meaning that the ClO_4^- diffusivity exceeds that of electron hopping in the DNA stack ($D_{APP,DNA}$ above), making an ionic atmosphere effect less plausible. On balance, the rates suggested here are in good agreement with those determined for related electron hops in well-defined oligonucleotides.[37]

It is interesting to consider how far electron hops proceed along a DNA strand. In a 1:1:1 (mole ratio) melt Co_{350}DNA + $Co_{350}(ClO_4)_2$ + $Fe_{350}(ClO_4)_2$, the total population of A + G sites equals that of the Fe (or Ru) complexes. The positive potential scan during a voltammogram like Figure 2 takes ca. 35 s, so for a M_{350}^{2+} with D_{PHYS} of 1.1×10^{-10} cm^2/s, the diffusion layer developed would be $\delta = (Dt)^{1/2} \approx 1$ μm. This distance from the 10 μm diameter working electrode would encompass 10 fmol of Fe or Ru complexes and an equal amount of base sites, which can be compared to the charge under the electrocatalytic wave of 4.2×10^{-9} coulombs or 44 fmol of electrons. This simple calculation shows that while the electrocatalytic wave is collected, all of the DNA base sites within a 1 μm profile (entire DNA strands of 1000 BP) can be consumed and each metal complex $M_{350}^{3+/2+}$ couple involved can turn over an average of three times. In addition, a considerable amount of DNA chains lying outside the profile can become oxidized by the base−base electron hopping process, which proceeds at a rate substantially greater than M_{350}^{3+} physical diffusion. Note that the above analysis assumes one-electron base oxidations, although multielectron oxidations

of DNA can occur in aqueous solution;[12−14,38] these multielectron reactions require exchange of protons, while the melts are relatively water-free.

We next return to the cyclic voltammetry of $Fe_{350}(ClO_4)_2$ and $Ru_{350}(ClO_4)_2$ melts from which the values of $k°$ and k_f used above were obtained through simulation fitting. These results are shown in Supporting Information (Figures S-2 and S-3). Figure S-2 shows observed and calculated voltammetry for the $Fe_{350}(ClO_4)_2$ complex (taken at a 5.1 μm radius Pt microelectrode at 67 °C) at two different potential scan rates of 75 and 50 mV/s. The D_{APP} was measured by chronoamperometry and a value of $R_{UNC} = 12.4$ MΩ from ac impedance measurements of melt ionic conductivity was used. The heterogeneous electron-transfer rate constant, $k° = 3.3 \times 10^{-4}$ cm/s and the rate constant for eq 4, $k_f = 0.085$ s^{-1} produced excellent fits at both scan rates. A similar analysis for $Ru_{350}(ClO_4)_2$ provided $k° = 2.1 \times 10^{-4}$ cm/s and $k_f = 0.34$ s^{-1} in Figure S-3. The similarity of the heterogeneous rate constants is unsurprising given that the D_{APP} values (8×10^{-9} and 6×10^{-9} cm^2/s for Fe and Ru, respectively) are also similar and reflect mainly the rates of homogeneous $M_{350}^{3+/2+}$ electron self-exchanges. The faster k_f in $Ru_{350}(ClO_4)_2$ is also unsurprising given its higher oxidizing potential.

Mass Transport of Nontailed Metal Complexes in DNA Molten Salts. As described in the Introduction, the interactions of intercalators with DNA have been used as a means of studying electron transport along the DNA helix.[17] We therefore added small concentrations (small because of the limited solubility) of the metal complexes $Os(bpy)_3Cl_2$ and $Os(bpy)_2(dppz)Cl_2$ (Figure 1) to the DNA melts to determine whether the dppz complex intercalated into DNA in the ionic liquid environment. A dramatically slower diffusivity of the dppz complex relative to the bpy complex would signal a strong binding interaction as observed in dilute aqueous solutions.[39] This binding difference has been observed electrochemically by measuring differences in aqueous solution diffusion coefficients of the two metal complexes in the presence of DNA.[39]

Figure 7A shows the voltammetry of $Os(bpy)_3Cl_2$ dissolved in a melt containing 1:4 (mole ratio) $Co_{350}DNA + Co_{350}(ClO_4)_2$. The concentrations in the melt are 2.5 mM, 0.41 M, and 0.16 M for $Os(bpy)_3Cl_2$, Co_{350}^{2+}, and DNA, respectively. The three waves (right to left) correspond to the $Co^{2+/1+}$ reduction and the $Co^{3+/2+}$ and $Os^{3+/2+}$ oxidations, at −0.50, 0.50, and 0.85 V vs AgQRE, respectively. As previously discussed, the currents for the $Co^{2+/1+}$ reduction are larger than those for the $Co^{3+/2+}$ oxidation, because of rapid $Co_{350}^{2+/1+}$ electron hopping that augments the rate of charge transport during the $Co_{350}^{2+/1+}$ reduction.[4,40] The electron hopping rate for the $Co_{350}^{3+/2+}$ reaction is too slow to enhance its charge transport diffusivity, and the concentration of the $Os(bpy)_3^{2+}$ complex is too small for it to engage in significant electron self-exchange enhancement of its charge transport. Also, the $Os(bpy)_3^{3+}$ complex is insufficiently oxidizing to react with the DNA bases. That is, the currents due to the $Os(bpy)_3^{2+}$ complex oxidation represent solely that of physical diffusion (D_{PHYS}) of that complex.

Measuring D_{PHYS} from Figure 7A is complicated by the combination of the small currents and the overlap with the $Co_{350}^{3+/2+}$ reaction. We therefore prepared melts in which $Co_{350}(ClO_4)_2$ was replaced with oxidatively silent $Ni_{350}(ClO_4)_2$.

Voltammetry at 67 °C of dilute $Os(bpy)_3^{2+}$ in a 1:3 (mole ratio) $Ni_{350}DNA + Ni_{350}(ClO_4)_2$ melt (Figure 7B) shows a two-electron $Ni_{350}^{2+/0}$ reduction[41] at −0.65 V and a much smaller but readily measured $Os^{3+/2+}$ oxidation (see inset). The slightly

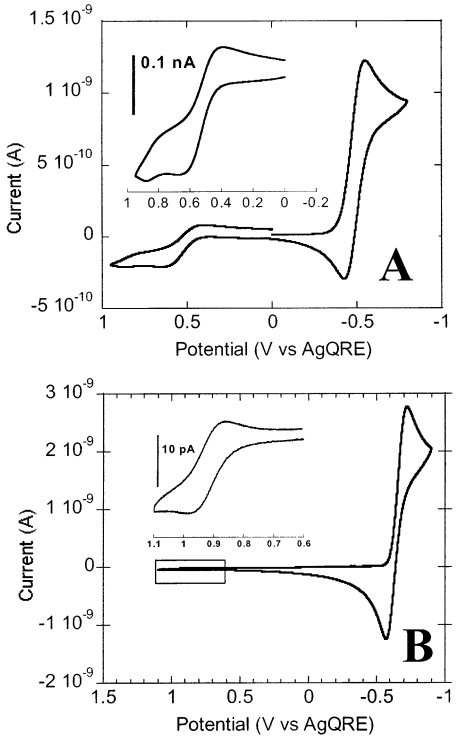

Figure 7. (A) Cyclic voltammetry of $Os(bpy)_2dppzCl_2$ in $Co_{350}DNA$ + 4 equiv of $Co_{350}(ClO_4)_2$. $[Os(bpy)_2dppz^{2+}] = 2.5$ mM, $[Co_{350}^{2+}]_{TOTAL} = 0.41$ M, and [DNA] = 0.16 M. (B) Cyclic voltammetry of $Os(bpy)_3Cl_2$ in $Ni_{350}DNA$ + 3 equiv $Ni_{350}(ClO_4)_2$. $[Os(bpy)_3^{2+}] = 3$ mM, $[Ni_{350}^{2+}] = 0.4$ M, and [DNA] = 0.2 M. All voltammetry measured at 67 °C on 5.6 μm radius Pt microelectrode at scan rate = 10 mV/s.

sigmoidal shape is attributed to partial radial diffusion at the 5.6-μm microelectrode.[42] The voltammetry of an analogous solution of $Os(bpy)_2(dppz)Cl_2$ in a 1:3 (mole ratio) $Ni_{350}DNA + Ni_{350}(ClO_4)_2$ melt is very similar to that in Figure 7B. Chronoamperometrically measured D_{PHYS} values for $Os(bpy)_3^{2+}$ and $Os(bpy)_2(dppz)^{2+}$ were practically identical: $(1.8 \pm 0.6) \times 10^{-8}$ and $(2.3 \pm 0.8) \times 10^{-8}$ cm^2/s, respectively. The similarity suggests that the two metal complexes possess similar DNA binding properties in the polyether environment. Undifferentiated binding was considered to be the result of either (1) an enhancement of the $Os(bpy)_3^{2+}$ binding to DNA in the polyether media relative to water or (2) loss of dppz intercalation in the melt. Measurement of $Os(bpy)_3^{2+}$ and $Os(bpy)_2(dppz)^{2+}$ D_{PHYS} in the $Co_{350}(ClO_4)_2$ melt (no DNA) showed that the diffusivity of the small molecules was entirely uninterrupted by the presence of the polyanion (Table S1 and Figure S4). This result was used to dismiss the possibility that charge interactions were predominant, and lack of intercalation was concluded. DNA intercalation in aqueous solution is driven by entropy and hydrophobic interactions; organized water molecules solvating the metal complex are freed while more favorable π-stacking interactions are realized when the ligand intercalates between the DNA base stack.[43] It appears that no such thermodynamic advantage occurs in the PEG-based melt environment.

Acknowledgment. We congratulate our colleague Prof. T. Baer on this wonderful occasion. This work was sponsored by the Department of Defense under Contract No. DAMD17-98-1-8224 (H.H.T.) and the Department of Energy (R.W.M.). We thank Dr. Stephen Feldberg of Brookhaven National Laboratories for many helpful discussions.

Supporting Information Available: Undiluted voltammetry of 3% $Os(bpy)_3Cl_2$ in $Co_{350}(ClO_4)_2$, digital simulations of $Co_{350}(ClO_4)_2$, $Ru_{350}(ClO_4)_2$, and EC reaction in Co_{350}DNA/$Fe_{350}(ClO_4)_2$ melt mixture. This material is available free of charge via the Internet at http://pubs.acs.org.

References and Notes

(1) (a) Velazquez, C. S.; Hutchison, J. E.; Murray, R. W. *J. Am. Chem. Soc.* **1993**, *115*, 7896 (b) Dickinson, E. V.; Williams, M. E.; Hendrickson, S. M.; Masui, H.; Murray, R. W. *J. Am. Chem. Soc.* **1999**, *121*, 613−616.

(2) Long, J. W.; Velazquez, C. S.; Murray, R. W. *J. Phys. Chem. A* **1996**, *100*, 5492−5499.

(3) Masui, H.; Murray, R. W. *Inorg. Chem.* **1997**, *36*, 5118.

(4) Williams, M. E.; Masui, H.; Long, J. W.; Malik, J.; Murray, R. W. *J. Am. Chem. Soc.* **1997**, *119*, 1997−2005.

(5) Kulesza, P. J.; Dickinson, E. V.; Williams, M. E.; Hendrickson, S. M.; Malik, M. A.; Miecznikowski, K.; Murray, R. W. *J. Phys. Chem. B* **2001**, *105*, 5833−5838.

(6) Leone, A. M.; Weatherly, S. C.; Williams, M. E.; Thorp, H. H.; Murray, R. W. *J. Am. Chem. Soc.* **2001**, *123*, 218−222.

(7) Leone, A. M.; Tibodeau, J. D.; Bull, S. H.; Thorp, H. H.; Murray, R. W. *J. Am. Chem. Soc.* **2003**, *125*, 6784−6790.

(8) Mirkin, C. A. *Inorg. Chem.* **2000**, *39*, 2258−2272.

(9) Elghanian, R.; Storhoff, J. J.; Mucic, R. C.; Letsinger, R. L.; Mirkin, C. A. *Science* **1997**, *277*, 1078−1081.

(10) (a) Adelman, L. M. *Science* **1994**, *266*, 1021−1024 (b) Pirrung, M. C.; Connors, R. V.; Odenbaugh, A. L.; Montague-Smith, M. P.; Walcott, N. G.; Tollett, J. J. *J. Am. Chem. Soc.* **2000**, *122*, 1873−1882 (c) Braich, R. S.; Chelyapov, N.; Johnson, C.; Rothemund, P. W. K.; Adleman, L. *Science* **2002**, *296*, 499−502.

(11) (a) Mirkin, C. A.; Taton, T. A. *Nature* **2000**, *405*, 626−627 (b) Fink, H. W.; Schonenberger, C. *Nature* **1999**, *398*, 407−410 (c) Porath, D.; Bezryadin, A.; de Vries, S.; Dekker: C. *Nature* **2000**, *403*, 635−638.

(12) (a) Johnston, D. H.; Glasgow, K. C.; Thorp, H. H. *J. Am. Chem. Soc.* **1995**, *117*, 8933−8938 (b) Armistead, P. M.; Thorp, H. H. *Anal. Chem.* **2001**, *73*, 558−564.

(13) Johnston, D. H.; Thorp, H. H. *J. Phys. Chem.* **1996**, *100*, 13837−13843.

(14) Armistead, P. M.; Thorp, H. H. *Anal. Chem.* **2000**, *72*, 3764−3770.

(15) (a) Eckhardt, A.; Espenhahn, E.; Napier, M.; Popovich, N.; Thorp, H.; Witwer, R. In *DNA Arrays: Technologies and Experimental Strategies*; Grigorenko, E. V., Ed.; CRC Press: Boca Raton, 2001; pp 39−60 (b) Horrocks, B. R.; Mirkin, M. V. *Anal. Chem.* **1998**, *70*, 4653−4660 (c) Taton, T. A.; Mirkin, C. A.; Letsinger, R. L. *Science* **2000**, *289*, 1757−1760 (d) He, L.; Musick, M. D.; Nicewarner, S. R.; Salinas, F. G.; Benkovic, S. J.; Natan, M. J.; Keating, C. D. *J. Am. Chem. Soc.* **2000**, *122*, 9071−9077 (e) Palecek, E.; Fojta, M. *Anal. Chem.* **2001**, *73*, 74A−83A (f) Reichert, J.; Csaki, A.; Koehler, J. M.; Fritzsche, W. *Anal. Chem.* **2000**, *72*, 6025−6029 (g) Wang, J.; Xu, D.; Polsky, R. *J. Am. Chem. Soc.* **2002**, *124*, 4208−4209 (h) Yu, C. J.; Wan, Y.; Yowanto, H.; Li, J.; Tao, C.; James, M. D.; Tan, C. L.; Blackburn, G. F.; Meade, T. J. *J. Am. Chem. Soc.* **2001**, *123*, 11155−11161 (i) Xu, X.-H.; Bard, A. J. *J. Am. Chem. Soc.* **1995**, *117*, 2627−2631 (j) Edman, C.; Raymond, D.; Wu, D.; Tu, E.; Sosnowski, R.; Butler, W.; Nerenberg, M.; Heller, M. *Nucleic Acids Res.* **1998**, *25*, 4907−4914 (k) Okahata, Y.; Kobayashi, T.; Tanaka, K.; Shimomura, M. *J. Am. Chem. Soc.* **1998**, *120*, 6165−6166 (l) Peterlinz, K. A.; Georgiadis, R. M.; Herne, T. M.; Tarlov, M. J. *J. Am. Chem. Soc.* **1997**, *119*, 3401−3402.

(16) (a) Lewis, F. D.; Liu, X.; Liu, J.; Miller, S. E.; Hayes, R. T.; Wasielewski, M. R. *Nature* **2000**, *406*, 51−53 (b) Gasper, S. M.; Schuster, G. B. *J. Am. Chem. Soc.* **1997**, *119*, 12762−12771 (c) Bixon, M.; Giese, B.; Wessely, S.; Langenbacher, T.; Michel-Beyerle, M. E.; Jortner, J. *Proc. Natl. Acad. Sci. U.S.A.* **1999**, *96*, 11713−11716.

(17) Arkin, M. R.; Stemp, E. D. A.; Holmlin, R. E.; Barton, J. K.; Hörmann, A.; Olson, E. J. C.; Barbara, P. F. *Science* **1996**, *273*, 475−480.

(18) (a) Wan, C.; Fiebig, T.; Schiemann, O.; Barton, J. K.; Zewail, A. H. *Proc. Natl. Acad. Sci. U.S.A.* **2000**, *97*, 14052−14055 (b) Schlag, E. W.; Yang, D.-Y.; Sheu, S.-Y.; Selzle, H. L.; Lin, S. H.; Rentzepis, P. M. *Proc. Natl. Acad. Sci. U.S.A.* **2000**, *97*, 9849−9854.

(19) Bard, A. J.; Faulkner, L. R. *Electrochemical Methods*, 2nd ed.; John Wiley and Sons: New York, 2001.

(20) Welch, T. W.; Corbett, A. H.; Thorp, H. H. *J. Phys. Chem.* **1995**, *99*, 11757−11763.

(21) (a) Burstall, F. H.; Dwyer, F. P.; Gyarfas, E. C. *J. Chem. Soc.* **1950**, 953−955 (b) DeSimone, R. E.; Drago, R. S. *J. Am. Chem. Soc.* **1970**, *92*, 2343−2352.

(22) (a) Laitinen, H. A. *Trans. Electrochem. Soc.* **1942**, *82*, 289 (b) Laitinen, H. A.; Kolthoff, I. M. *J. Am. Chem. Soc.* **1939**, *61*, 3344.

(23) Rudolph, M.; Reddy, D. P.; Feldberg, S. W. *Anal. Chem.* **1994**, *66*, 589a.

(24) (a) Gary, F. M. *Solid Polymer Electrolytes, Fundamentals and Technological Applications*; VCH Publishers: New York, 1991 (b) MacCallum, J. R.; Vincent, C. A. *Polymer Electrolyte Reviews*; Elsevier Applied Science: Oxford, U.K., 1989; Vol. 1 and 2.

(25) Weatherly, S. C.; Yang, I. V.; Armistead, P. A.; Thorp, H. H. *J. Phys. Chem. B* **2003**, *107*, 372−378.

(26) (a) Maeder, M.; Zuberbühler, A. D. *Anal. Chem.* **1990**, *62*, 2220. (b) The initial concentrations of Fe^{2+} and Fe^{3+} were determined from the stopped-flow data. $[Fe^{2+}] = A_{min}/b\epsilon_{Fe^{2+}}$ and $[Fe^{3+}] = A_{max} - A_{min}/b\epsilon_{Fe^{2+}}$, where A_{max} is the maximum absorbance at the wavelength of interest, A_{min} is the minimum absorbance, b is the cell path length (1.8 cm), and $\epsilon_{Fe^{2+}}$ is the extinction coefficient (27 800 M^{-1} cm^{-1}) for Fe^{2+}.

(27) (a) Yang, I. V.; Thorp, H. H. *Inorg. Chem.* **2000**, *39*, 4969−4976 (b) Weatherly, S. C.; Yang, I. V.; Thorp, H. H. *J. Am. Chem. Soc.* **2001**, *123*, 1236−1237.

(28) (a) Marcus, R. A.; Sutin, N. *Biochim. Biophys. Acta* **1985**, *811*, 265−322 (b) Barbara, P. F.; Meyer, T. J.; Ratner, M. A. *J. Phys. Chem.* **1996**, *100*, 13148−13168.

(29) Nicholson, R. S.; Shain, I. *Anal. Chem.* **1964**, *36*, 706−735.

(30) Lee, D.; Harper, A. S.; DeSimone, J. M.; Murray, R. W. *J. Am. Chem. Soc.* **2002**, *125*, 1096−1103.

(31) The value for the M_{350}^{3+-}DNA electron-transfer rate was varied from 10 to 1×10^4 M^{-1} s^{-1} with little effect on the simulation. $k_1 = 700$ M^{-1} s^{-1} was used to generated the simulation in Figure 6 to maintain consistency with the simulations in other figures.

(32) Majda, M. In *Molecular Design of Electrode Surfaces*; Murray, R. W., Ed.; John Wiley and Sons: New York, 1992; p 159.

(33) (a) While a simplification, we assumed equal probability of all four hops and center-to-center separation of bases to be 10 Å—one-half the diameter of the double helix. (b) Watson, J. D.; Crick, F. H. C. *Nature* **1953**, *171*, 737−738.

(34) Treadway, C. R.; Hill, M. G.; Barton, J. K. *Chem. Phys.* **2002**, *281*, 409−428.

(35) Marcus, R. A. *J. Phys. Chem. B* **1998**, *102*, 10071−10077.

(36) Lee, D.; John, C. H.; Leone, A. M.; DeSimone, J. M.; Murray, R. W. *J. Am. Chem. Soc.* **2002**, *124*, 9310−9317.

(37) (a) Lewis, F. D.; Zuo, X.; Liu, J.; Hayes, R. T.; Wasielewski, M. *J. Am. Chem. Soc.* **2002**, *124*, 4568−4569 (b) Barnett, R. N.; Cleveland, C. L.; Landman, U.; Boone, E.; Kanvah, S.; Schuster, G. B. *J. Phys. Chem.* **2003**, *107*, 3525−3537.

(38) Burrows, C. J.; Muller, J. G. *Chem. Rev.* **1998**, *98*, 1109−1151.

(39) (a) Welch, T. W.; Thorp, H. H. *J. Phys. Chem.* **1996**, *100*, 13829−13836 (b) Carter, M. T.; Bard, A. J. *J. Am. Chem. Soc.* **1987**, *109*, 7528−7530 (c) Carter, M. T.; Rodriguez, M.; Bard, A. J. *J. Am. Chem. Soc.* **1989**, *111*, 8901.

(40) (a) Kaufman, F. B.; Engler, E. M. *J. Am. Chem. Soc.* **1979**, *101*, 547−549 (b) Buttry, D. A.; Anson, F. C. *J. Am. Chem. Soc.* **1983**, *105*, 685−689.

(41) (a) Bartlett, P. N.; Easstwick-Field, B. *Electrochim. Acta* **1993**, *38*, 2215−2523 (b) Henne, B. J.; Bartak, D. E. *Inorg. Chem.* **1984**, *23*, 369−373.

(42) (a) Wightman, R. M. *Anal. Chem.* **1981**, *53*, 1125A−1134A (b) The approximate diffusion layer thickness is 3 μm (from $(2Dt)^{1/2}$) at a scan rate of 10 mV/s and $D_{PHYS} = 1.8 \times 10^{-8}$ cm^2/s measured by chronoamperometry.

(43) Friedman, A. E.; Chambron, J. C.; Sauvage, J. P.; Turro, N. J.; Barton, J. K. *J. Am. Chem. Soc.* **1990**, *112*, 4960.